

**AN EVALUATION OF OIL PALM EMPTY FRUIT
BUNCH LIGNIN ON SELECTED PHASE II DRUG
METABOLIZING ENZYMES**

NORLIYANA MOHD SALLEH

**UNIVERSITI SAINS MALAYSIA
2016**

**AN EVALUATION OF OIL PALM EMPTY FRUIT
BUNCH LIGNIN ON SELECTED PHASE II DRUG
METABOLIZING ENZYMES**

by

NORLIYANA MOHD SALLEH

**Thesis submitted in fulfillment of the requirements
for the degree of
Doctor of Philosophy**

September 2016

ACKNOWLEDGEMENT

First and foremost all praise be to Allah, the Almighty, the Benevolent for His blessing and guidance for giving me the patience and facilitate the completion of my study. I would like to express my appreciation to my supervisors, Prof. Dr. Sabariah Ismail and Assoc. Prof. Dr. Mohamad Nasir Mohamad Ibrahim for their consistent support, guidance and advice throughout the completion of this work. Also, I would like to express my gratitude to Prof. Dr. Sharif Mahsufi Mansor, Director of Centre for Drug Research, Universiti Sains Malaysia, for giving me the opportunity to continue my study in this Centre and also providing me with facilities vital to the completion of my study.

My sincere gratitude also goes to Prof. Nicolas Brosse from the LERMAB in Université Henri Poincaré, France for his help in accomplishing the characterization part from this study. Thank you also to technical staff from LERMAB, Université Henri Poincaré, France, School of Chemical Sciences and Centre for Drug Research Universiti Sains Malaysia. A special thanks to all of them for their much appreciated help.

I would like to acknowledge the financial support from Ministry of Education for the MyPhD scholarship; financial support and opportunity from SDCC AIT France network for 3 months research program in LERMAB, Université Henri Poincaré, France.

Finally, my heartfelt appreciation goes to my parents, family and friends, who have assisted me in various aspects and have continuously given me much needed support and encouragement. Thank you very much.

TABLE OF CONTENTS

Acknowledgment	ii	
Tables of Contents	iii	
List of Tables	xi	
List of Figures	xiv	
List of Symbols	xxvi	
List of Abbreviations	xxvii	
List of Appendices	xxix	
Abstrak	xxx	
Abstract	xxxiii	
CHAPTER 1	INTRODUCTION	1
1.1	Background of the study	1
1.2	Problem statement	4
CHAPTER 2	LITERATURE REVIEW	7
2.1	Oil palm empty fruit bunch	7
2.2	Oil palm empty fruit bunch lignin	8
2.3	The applications of lignin for pharmaceutical and food industry	13
2.3.1	The potential of oil palm EFB lignin as an emulsifying agent for oil in water system emulsion	13
2.3.2	Lignin-based formulation (Ligmed-A) as antidiarrheal drug	15
2.3.3	Antioxidant properties of lignin	15
2.4	Drug metabolizing enzymes	18

2.5	UDP-glucuronosyltransferase enzymes activity	20
2.6	Glutathione S-transferase enzymes activity	24
2.7	Enzyme sources of drug metabolism	26
2.8	Current approaches use to study drug metabolism interaction	29
2.9	Enzymes kinetics	30
2.9.1	Enzyme inhibition kinetics	32
2.9.1(a)	Competitive inhibition	33
2.9.1(b)	Non-competitive inhibition	35
2.9.1(c)	Un-competitive inhibition	36
2.9.1(d)	Mixed-type inhibition	38
2.9.2	The inhibitor constant, K_i	40
CHAPTER 3 MATERIALS AND METHODS		41
3.1	Materials, chemicals and reagents	41
3.2	Experimental design	42
3.3	Soda, kraft and organosolv pulping process	44
3.4	Preparation of soda, kraft and organosolv oil palm EFB lignin	44
3.5	Purification of oil palm EFB Lignin	45
3.6	Characterization of oil palm EFB lignin	45
3.6.1	Fourier transform infrared (FT-IR) spectroscopy analysis of oil palm EFB lignin	45
3.6.2	Carbon-13 NMR spectroscopy (^{13}C NMR) analysis of oil palm EFB lignin	46
3.6.3	Phosphorus-31 NMR spectroscopy (^{31}P NMR) analysis of oil palm EFB lignin	46
3.6.4	Gel permeation chromatography (GPC) analysis	46
3.6.5	Total flavonoids content analysis	47

3.6.6	Nitrobenzene oxidation process of oil palm EFB lignin	48
3.6.7	High performance liquid chromatography analysis (HPLC) of oil palm EFB lignin	48
3.6.8	Determination of DPPH scavenging capacity of oil palm EFB lignin	49
3.7	Preparation of stock and working solutions of positive inhibitors (diclofenac and tannic acid), oil palm EFB lignin (soda, kraft and organosolv) and pure compounds (vanillin, syringaldehyde and p-hydroxybenzaldehyde)	50
3.8	Source of animals	50
3.8.1	<i>In vitro</i> treatment	51
3.8.2	<i>In vivo</i> treatment	51
3.9	Preparation of rat liver and kidney microsomes and cytosolic fraction	52
3.10	Determination of protein concentration of rat liver and kidney microsomes and cytosolic fraction	53
3.11	Para-nitrophenol (<i>p</i> -NP) glucuronidation assay of rat liver microsome (RLM) and rat kidney microsome (RKM)	53
3.11.1	Preparation of <i>p</i> -nitrophenol (<i>p</i> -NP) standard curve	54
3.11.2	Optimization of incubation time for <i>p</i> -NP glucuronidation assay	54
3.11.3	Optimization of protein concentration for <i>p</i> -NP glucuronidation assay	55
3.11.4	Optimization of Triton X-100 for <i>p</i> -NP glucuronidation assay	56
3.11.5	Determination of maximal velocity of reaction (V_{\max}) and Michaelis Constant (K_m) value	57
3.11.6	Determination of organic solvent on <i>p</i> -nitrophenol (<i>p</i> -NP) glucuronidation assay	57
3.11.7	The effect of diclofenac (positive inhibitor), oil palm EFB lignin and its main oxidative compounds on p-nitrophenol (<i>p</i> -NP) glucuronidation assay in rat liver	58

	microsomes (RLM) and rat kidney microsomes (RKM) by <i>in vitro</i> treatment	
3.11.8	The effect of oil palm EFB lignin on <i>p</i> -nitrophenol (<i>p</i> -NP) glucuronidation assay in rat liver microsome (RLM) and rat kidney microsomes (RKM) by <i>in vivo</i> treatment	59
3.11.9	Calculation of UGT specific activity towards <i>p</i> -NP in RLM and RKM	60
3.12	4-methylumbelliferone (4-MU) glucuronidation assay of rat liver microsome (RLM) and rat kidney microsome (RKM)	61
3.12.1	Preparation of 4-methylumbelliferone-glucuronide (4-MUG) standard curve	62
3.12.2	Optimization of incubation time for 4-MU glucuronidation assay	62
3.12.3	Optimization of protein concentration for 4-MU glucuronidation assay	63
3.12.4	Optimization of Triton X-100 for 4-MU glucuronidation assay	63
3.12.5	Determination of maximal velocity of reaction (V_{max}) and Michaelis Constant (K_m) value for 4-MU glucuronidation assay	64
3.12.6	Determination of maximal velocity of reaction (V_{max}), Michaelis constant (K_m) value, intrinsic clearance (CL_{int}), inhibition constant (K_i) and mode inhibition in an inhibitor concentration-dependent	65
3.12.7	Effect of organic solvent on 4-methylumbelliferone (4-MU) glucuronidation assay	66
3.12.8	Inhibitory effect of diclofenac (positive inhibitor), oil palm EFB lignin and its main oxidative compounds on 4-methylumbelliferone (4-MU) glucuronidation assay in rat liver microsome (RLM) and rat kidney microsomes (RKM)	67
3.12.9	The effect of oil palm EFB lignin on 4-methylumbelliferone (4-MU) glucuronidation assay in rat liver microsome (RLM) and rat kidney microsomes (RKM) by <i>in vivo</i> treatment	68
3.12.10	Determination of maximal velocity of reaction (V_{max}), Michaelis constant (K_m) value, intrinsic clearance	69

	(CL _{int}) for 4-MU glucuronidation assay	
3.12.11	High performance liquid chromatography conditions	69
3.12.12	Calculation of 4-MU UGT activity in RLM and RKM	70
3.13	Glutathione S-transferase (GST) enzymes activity assay	70
3.13.1	Optimization of time and protein concentration for glutathione S-transferase enzymes activity assay	71
3.13.2	Determination of maximal velocity of reaction (V_{max}) and Michaelis constant (K_m) value for GST assay	71
3.13.3	Determination of organic solvent on GST assay	72
3.13.4	The effect of tannic acid (positive inhibitor), oil palm EFB lignin and its main oxidative compounds on glutathione S-transferase (GST) enzyme activity assay in rat liver cytosolic fractions (RLC) and rat kidney cytosolic fractions (RKC) by <i>in vitro</i> treatment	73
3.13.5	The effect of oil palm EFB lignin and its main oxidative compounds on glutathione-S-transferase (GST) enzyme activity assay in rat liver cytosolic (RLC) and rat kidney cytosolic (RKC) by <i>in vivo</i> treatment	74
3.13.6	Calculation of GST specific activity in rat liver and rat kidney cytosolic fractions	75
3.14	Statistical analysis	76
3.15	Data analysis	76
CHAPTER 4	RESULTS AND DISCUSSION	77
4.1	Characterization of Oil Palm Empty Fruit Bunch (EFB) Lignin	77
4.1.1	Fourier transform infrared (FT-IR) spectroscopy analysis of oil palm EFB lignin	77
4.1.2	Carbon-13 nuclear magnetic resonance (¹³ C NMR) analysis of oil palm EFB lignin	81
4.1.3	Phosphorus-31 nuclear magnetic resonance (³¹ P NMR) analysis of soda, kraft and organosolv oil palm EFB lignin	85
4.1.4	Molecular weight distribution of soda, kraft and organosolv oil palm EFB lignin	88

4.1.5	Total flavonoids content of soda, kraft and organosolv oil palm EFB lignin	89
4.1.6	High performance liquid chromatography (HPLC) analysis of soda, kraft and organosolv oil palm EFB lignin	91
4.1.7	Radical scavenging activity of soda, kraft and organosolv oil palm EFB lignin	96
4.2	The Effect of Oil Palm EFB Lignin and Its Main Oxidative Compounds on Rat Liver and Kidney Microsomes Glucuronidation of <i>p</i> -nitrophenol by <i>In Vitro</i> Treatment	100
4.2.1	Protein concentration determination	100
4.2.2	Optimization of <i>p</i> -NP glucuronidation in rat liver microsomes (RLM) and rat kidneys microsomes (RKM)	100
4.2.2(a)	Linearity of incubation time	101
4.2.2(b)	Linearity of protein concentration	102
4.2.2(c)	Optimization of Triton X-100 concentration	103
4.2.2(d)	Determination of K_m and V_{max} Values	104
4.2.3	The effect of organic solvent on <i>p</i> -NP glucuronidation	105
4.2.4	The effect of diclofenac (positive inhibitor), oil palm EFB lignin and its main oxidative compounds on <i>p</i> -nitrophenol (<i>p</i> -NP) glucuronidation in rat liver microsome (RLM) and rat kidneys microsomes (RKM)	106
4.3	The Effect of Oil Palm EFB Lignin on Rat Liver and Kidney Microsomes Glucuronidation of <i>p</i> -nitrophenol by <i>In Vivo</i> Treatment	117
4.3.1	Protein concentration determination	117
4.3.2	The effect of oil palm EFB lignin on <i>p</i> -NP glucuronidation in rat liver microsomes (RLM) and rat kidney microsomes (RKM) by <i>in vivo</i> treatment	119
4.4	The Effect of Oil Palm EFB Lignin and Its Main Oxidative Compounds on Rat Liver and Kidney Microsomes Glucuronidation of 4-Methylumbelliferone by <i>In Vitro</i> Treatment	124
4.4.1	Protein concentration determination	124
4.4.2	High performance liquid chromatography analysis of 4-	125

	methylumbelliferone glucuronide	
4.4.3	Optimization of 4-MU glucuronidation in rat liver microsomes (RLM) and rat kidneys microsomes (RKM)	126
4.4.3(a)	Linearity of incubation time	127
4.4.3(b)	Linearity of protein concentration	128
4.4.3(c)	Optimization of Triton X-100 concentration	128
4.4.3(d)	Determination of K_m and V_{max}	130
4.4.4	The effect of organic solvent on 4-MU glucuronidation	131
4.4.5	The effect of diclofenac (positive inhibitor), oil palm EFB lignin and its main oxidative compounds on 4-methylumbelliferone (4-MU) glucuronidation in rat liver microsome (RLM) and rat kidney microsomes (RKM) by <i>in vitro</i> treatment	132
4.4.6	The effect of soda oil palm EFB lignin on Michaelis Menten kinetics of 4-MU glucronidation in RLM by <i>in vitro</i> treatment	142
4.5	The Effect of Oil Palm EFB Lignin on Rat Liver and Kidney Microsomes Glucuronidation of 4-Methylumbelliferone (4MU) by <i>In Vivo</i> Treatment	145
4.5.1	Protein concentration determination	145
4.5.2	The effect of oil palm EFB lignin on 4-MU glucuronidation in rat liver microsomes (RLM) and rat kidney microsomes (RKM) by <i>in vivo</i> treatment	146
4.5.3	The effect of oil Palm EFB lignin on Michaelis Menten kinetics of 4-MU glucuronidation by <i>in vivo</i> treatment	152
4.6	The Effect of Oil Palm EFB Lignin and Its Main Oxidative Compounds on Glutathione S-Transferase (GST) Activity in Rat Liver and Kidney Cytosolic Fraction by <i>In Vitro</i> Treatment	155
4.6.1	Protein concentration determination	155
4.6.2	Optimization of GST in rat liver cytosolic fraction (RLC) and rat kidney cytosolic fraction (RKC)	155
4.6.2(a)	Linearity of incubation time and protein concentration	156

4.6.2(b)	Determination of K_m and V_{max} Values	158
4.6.3	The effect of organic solvent on GST enzyme activity	159
4.6.4	The effect of tannic acid (positive inhibitor), oil palm EFB lignin and its main oxidative compounds on GST enzyme activity in RLC and RKC by <i>in vitro</i> treatment	160
4.7	The Effect of Oil Palm EFB Lignin on Glutathione S-Transferase (GST) Enzyme Activity in Rat Liver Cytosolic Fraction (RLC) and Rat Kidney Cytosolic Fraction (RKC) by <i>In Vivo</i> Treatment	170
4.7.1	Protein concentration determination	170
4.7.2	The effect of oil palm EFB lignin on GST enzyme activity in RLC and RKC by <i>in vivo</i> treatment	172
CHAPTER 5	CONCLUSION	179
	REFERENCES	184
	APPENDICES	207
	LIST OF PUBLICATIONS	215

LIST OF TABLES

		Page
Table 4.1	Assignments and absorption bands for soda, kraft and organosolv oil palm EFB lignin	80
Table 4.2	Signal assignment in ^{13}C NMR spectrum of soda, kraft and organosolv oil palm EFB lignin	84
Table 4.3	Lignin extracted from oil palm EFB characteristics calculated from ^{31}P NMR data	85
Table 4.4	Weight-average (M_w), number average (M_n) and polydispersity (M_w/M_n) of soda, kraft and organosolv oil palm EFB lignin	88
Table 4.5	Total flavonoids content in oil palm EFB lignin. Results expressed as mean \pm SD	90
Table 4.6	Intra- and inter-day precision (% RSD) for compounds from alkaline nitrobenzene oxidation of oil palm EFB lignin (triplicates per day for five days)	92
Table 4.7	The yield (% (w/w) dry sample) of compounds from alkaline nitrobenzene oxidation of oil palm EFB lignin. Results are expressed as mean \pm SD (n=3).	94
Table 4.8	The 50% inhibition values (IC_{50}) of DPPH radical scavenging of oil palm EFB lignin compared to ascorbic acid. Results are expressed as mean in microgram per milliliter ($\mu\text{g mL}^{-1}$) \pm SD for three replicates (n=3).	96
Table 4.9	The half maximal inhibitory concentration (IC_{50}) values of oil palm EFB lignin and its main oxidative compounds on the <i>p</i> -NP UGT activity in RLM and RKM. Data are expressed as the best-fit IC_{50} values \pm SD for five replicates (n=5).	116

Table 4.10	Protein concentration of microsomes in male Sprague Dawley rats liver and kidneys treated orally for 14 days with oil palm EFB lignin. The values were expressed as the mean concentration \pm SD for three replicates (n=3). Statistical analysis was conducted using Dunnet's test. * indicates significant difference from control (received co-solvent) ($p < 0.05$).	118
Table 4.11	The <i>p</i> -NP UGT activity in RLM and RKM. Rats were treated with 0, 40 and 400 mg kg ⁻¹ of soda, kraft and organosolv oil palm EFB lignin for 14 days before sacrifice. Values are mean of UGT specific activity \pm SD for five replicates. Statistical analysis was conducted using one-way ANOVA followed by Dunnet's test. * indicates significant difference from control (received co-solvent) ($p < 0.05$).	122
Table 4.12	The half maximal inhibitory concentration (IC ₅₀) values of oil palm EFB lignin and its main oxidative compounds on the 4-MU UGT activity in RLM and RKM. Data are expressed as the best-fit IC ₅₀ values \pm SD for three replicates (n=3).	141
Table 4.13	Kinetics parameters for 4-MU glucuronidation in concentration-dependents of soda oil palm EFB lignin. Data represents the mean values \pm SD for three replicates (n=3). Statistical analysis was conducted using one-way ANOVA followed by Dunnet's test. * indicates significant difference from control (without inhibitor) ($p < 0.05$).	145
Table 4.14	The 4-MU UGT activity in RLM and RKM. Rats were treated with 0, 40 and 400 mg kg ⁻¹ of soda, kraft and organosolv oil palm EFB lignin for 14 days before sacrifice. Values are mean of UGT specific activity \pm SD for three replicates. Statistical analysis was conducted using one-way ANOVA followed by Dunnet's test. * indicates significant difference from control (received co-solvent) ($p < 0.05$).	150

Table 4.15	Effect of 400 mg oil palm EFB lignin mg per kg rat <i>in vivo</i> treatment on K_m , V_{max} and CL_{int} of RLM and RKM glucuronidation. Values are mean \pm SD for three replicates (n=3). Statistical analysis was conducted using one-way ANOVA followed by Dunnet's test. * indicates significant difference from control (received co-solvent) ($p < 0.05$).	154
Table 4.16	The half maximal inhibitory concentration (IC_{50}) values of oil palm EFB lignin and its main oxidative compounds on the GST enzyme activity in RLC and RKC. Data are expressed as the best-fit IC_{50} values \pm SD for five replicates (n=5).	170
Table 4.17	Protein concentration in RLC and RKC treated orally for 14 days with oil palm EFB lignin. Statistical analysis was conducted using one-way ANOVA followed by Dunnet's test. * indicates significant difference from control (received co-solvent) ($p < 0.05$).	171
Table 4.18	The GST enzyme activity in RLC and RKC. Rats were treated with 0, 40 and 400 mg kg^{-1} of soda, kraft and organosolv oil palm EFB lignin for 14 days before sacrifice. Values are mean of GST specific activity \pm SD for five replicates (n=5). Statistical analysis was conducted using one-way ANOVA followed by Dunnet's test. * indicates significant difference from control (received co-solvent) ($p < 0.05$).	178

LIST OF FIGURES

		Page
Figure 2.1	Lignin position in vascular plant (Lewis and Yamamoto, 1990)	9
Figure 2.2	Lignin consist of three major phenylpropanoid units which are (a) trans- <i>p</i> -coumaryl alcohol, (b) trans-coniferyl alcohol and (c) trans-sinapyl alcohol (Lewis and Yamamoto, 1990)	9
Figure 2.3	Flowchart of the production of paper and lignin from oil palm empty fruit bunch	11
Figure 2.4	Conjugation of a nucleophilic substrate with uridine 5'-diphospho- α -D-glucuronic acid (UDPGA), X is define as hydroxyl, carboxyl, carbonyl, sulfhydryl or amine (adopted from Rowland et al., 2013).	22
Figure 2.5	Formation of glutathione conjugate (adopted from Jancova et al., 2010)	25
Figure 2.6	Plot of the reaction velocity (V) as a function of the substrate concentration [S] for an enzyme that obeys Michaelis-Menten kinetics shows that the maximal velocity (V_{\max}) is approached asymptotically. The Michaelis constant (K_m) is the substrate concentration yielding a velocity of $\frac{1}{2} V_{\max}$.	32
Figure 2.7	The Lineweaver-Burk reciprocal plot for the set of data shows a series of lines crossing the y ($1/v$) axis at the same point (V_{\max} unchanged, K_m increased) in the presence of the inhibitor.	34
Figure 2.8	The Lineweaver-Burk reciprocal plot for the set of data shows a series of lines crossing the x ($1/[S]$) axis at the same point (V_{\max} changed, K_m unchanged) in the presence of the inhibitor.	36
Figure 2.9	The Lineweaver-Burk reciprocal plot for the set of data shows a series of lines crossing the y ($1/v$) and x ($1/[S]$) axis at the different point (V_{\max} changed, K_m changed) in the presence of the inhibitor.	38

Figure 2.10	The Lineweaver-Burk reciprocal plot for the set of data shows a series of lines crossing the y ($1/v$) and x ($1/[S]$) axis at the different point (V_{\max} changed, K_m changed). The plots display a nest of lines that intersect above the x -axis in the presence of the inhibitor.	39
Figure 2.11	The Theoretical secondary plot of the slopes of Lineweaver-Burk plot at various inhibitor concentrations. The value of K_i can be determined from the negative value of the x -intercept of this type of plot, $[I]$ is the inhibitor concentration.	40
Figure 3.1	Experimental design for the effects of oil palm EFB lignin and its main oxidation compounds on phase II drug metabolizing enzymes	43
Figure 4.1	FT-IR spectra of soda, kraft and organosolv oil palm EFB lignin	79
Figure 4.2	Quantitative ^{13}C NMR spectrum of oil palm EFB lignin a) organosolv b) soda and c) kraft	82
Figure 4.3	Representation of a coumarylated lignin fragment at the γ position (El Hage et al., 2009)	83
Figure 4.4	Quantitative ^{31}P NMR spectra of A: Organosolv B: Soda and C: Kraft oil palm EFB lignin	87
Figure 4.5	A basic structure of diphenylpropane (Kumar and Pandey, 2013)	89
Figure 4.6	HPLC chromatogram for standard compounds A: hydroxybenzoic acid; B: vanillic acid; C: syringic acid; D: <i>p</i> -hydroxybenzaldehyde; E: vanillin; F: <i>p</i> -coumaric acid; G: syringaldehyde; H: ferulic acid	93
Figure 4.7	Compounds A: hydroxybenzoic acid; B: vanillic acid; C: syringic acid; D: <i>p</i> -hydroxybenzaldehyde; E: vanillin; F: <i>p</i> -coumaric acid (not detected); G: syringaldehyde; H: ferulic acid) that found in (a) soda (b) kraft and (c) organosolv oil palm EFB lignin.	95

Figure 4.8	DPPH scavenging activities of soda, kraft and organosolv oil palm EFB lignin compare with ascorbic acid. Results are expressed as percent of mean \pm SD (n=3).	97
Figure 4.9	Trapping and stabilization of radicals by lignin (Barclay et al., 1997).	99
Figure 4.10	The effect of incubation time on <i>p</i> -NP glucuronide formation in RLM and RKM. Reactions were performed in the presence of <i>p</i> -NP (500 μ M) and RLM or RKM (0.5 mg mL ⁻¹) in a total volume incubation of 0.2 mL at 37 °C. Each point represents the mean <i>p</i> -NP glucuronidated (μ M) values \pm SD for triplicates (n=3).	101
Figure 4.11	The effect of RLM and RKM protein concentration on <i>p</i> -NP glucuronide formation in RLM and RKM. Reactions were performed in the presence of <i>p</i> -NP (500 μ M) for 30 minutes incubation time in a total volume incubation of 0.2 mL at 37 °C. Each point represents the mean <i>p</i> -NP glucuronidated (μ M) values \pm SD for triplicates (n=3).	102
Figure 4.12	The effect of Triton X-100 concentration on <i>p</i> -NP glucuronide formation in RLM and RKM. Reactions were performed in the presence of <i>p</i> -NP (500 μ M), RLM or RKM (0.125 mg mL ⁻¹) for 30 minutes incubation time in a total volume incubation of 0.2 mL at 37 °C. Each point represents the mean <i>p</i> -NP glucuronidated (μ M) values \pm SD for triplicates (n=3).	103
Figure 4.13	Michaelis-Menten plot for <i>p</i> -NP glucuronidation in RLM and RKM, respectively. Each reaction (200 μ L) was performed in the presence of RLM or RKM (0.125 mg mL ⁻¹) and <i>p</i> -NP concentration range from 50 – 3000 μ M. Each point represents the mean of nmol per minute per milligram of <i>p</i> -NP glucuronide formed \pm SD of three replicates (n=3).	105
Figure 4.14	Effect of DMSO on <i>p</i> -NP glucuronidation in RLM and RKM. The reaction was performed in the presence of <i>p</i> -NP (0.5 mM), RLM or RKM (0.125 mg mL ⁻¹) at five different concentrations of DMSO. Each bar represents the mean percentage activity relative to control \pm SD for five replicates (n=5). Statistical analysis was conducted using one-way ANOVA followed by Dunnet's test. * indicates significant difference from control (without DMSO) (p < 0.05).	106

- Figure 4.15 Effect of soda, kraft and organosolv on *p*-NP glucuronidation in RLM. The reaction was performed in the presence of *p*-NP (0.5 mM), RLM (0.125 mg mL⁻¹) at six different concentrations of oil palm EFB lignin. Each bar represents the mean percentage activity relative to negative control ± SD for five replicates (n=5). Statistical analysis was conducted using one-way ANOVA followed by Dunnet's test. * indicates significant difference from control (without inhibitor) (p < 0.05). 103
- Figure 4.16 Inhibition of *p*-NP glucuronidation in RLM by soda and kraft oil palm EFB lignin compared to positive inhibitor (diclofenac). Data are expressed as the mean percentage activity relative to negative control ± SD for five replicates (n=5). Error bars represent two-sided standard error of the mean. Data points were fitted to IC₅₀ equation as described under Materials and Methods. Goodness of fit R² values were greater than 0.9. 108
- Figure 4.17 Effect of soda, kraft and organosolv on *p*-NP glucuronidation in RKM. The reaction was performed in the presence of *p*-NP (0.5 mM), RKM (0.125 mg mL⁻¹) at five different concentrations of oil palm EFB lignin. Each bar represents the mean percentage activity relative to negative control ± SD for five replicates (n=5). Statistical analysis was conducted using one-way ANOVA followed by Dunnet's test. * indicates significant difference from control (without inhibitor) (p < 0.05). 109
- Figure 4.18 Inhibition of *p*-NP glucuronidation in RKM by soda and kraft oil palm EFB lignin compared to positive inhibitor (diclofenac). Data are expressed as the mean percentage activity relative to control ± SD for five replicates (n=5). Error bars represent two-sided standard error of the mean. Data points were fitted to IC₅₀ equation as described under Materials and Methods. Goodness of fit R² values were greater than 0.9. 110
- Figure 4.19 Effect of vanillin, syringaldehyde and kraft and *p*-hydroxybenzaldehyde on *p*-NP glucuronidation in RLM. The reaction was performed in the presence of *p*-NP (0.5 mM), RLM (0.125 mg mL⁻¹) at six different concentrations of oil palm EFB lignin. Each bar represents the mean percentage activity relative to negative control ± SD for five replicates (n=5). Statistical analysis was conducted using one-way ANOVA followed by 113

Dunnet's test. * indicates significant difference from control (without inhibitor) ($p < 0.05$).

- Figure 4.20 Effect of vanillin, syringaldehyde and *p*-hydroxybenzaldehyde on *p*-NP glucuronidation in RKM. The reaction was performed in the presence of *p*-NP (0.5 mM), RKM (0.125 mg mL⁻¹) at five different concentrations of oil palm EFB lignin. Each bar represents the mean percentage activity relative to negative control \pm SD for five replicates (n=5). Statistical analysis was conducted using one-way ANOVA followed by Dunnet's test. * indicates significant difference from control (without inhibitor) ($p < 0.05$). 113
- Figure 4.21 Inhibition of *p*-NP glucuronidation in RLM by vanillin and syringaldehyde compared to positive inhibitor (diclofenac). Data are expressed as the mean percentage activity relative to negative control \pm SD for five replicates (n=5). Error bars represent two-sided standard error of the mean. Data points were fitted to IC₅₀ equation as described under Materials and Methods. Goodness of fit R² values were greater than 0.9. 114
- Figure 4.22 Inhibition of *p*-NP glucuronidation in RKM by vanillin and syringaldehyde compared to positive inhibitor (diclofenac). Data are expressed as the mean percentage activity relative to negative control \pm SD for five replicates (n=5). Error bars represent two-sided standard error of the mean. Data points were fitted to IC₅₀ equation as described under Materials and Methods. Goodness of fit R² values were greater than 0.9. 115
- Figure 4.23 Effect of soda, kraft and organosolv on *p*-NP glucuronidation by *in vivo* treatment in RLM. Rats were treated with 0, 40 and 400 mg kg⁻¹ of soda, kraft and organosolv oil palm EFB lignin for 14 days before sacrifice. Each bar represents the mean percentage activity relative to control \pm SD for five replicates (n=5). Statistical analysis was conducted using one-way ANOVA followed by Dunnet's test. * indicates significant difference from control (received co-solvent) ($p < 0.05$). 120
- Figure 4.24 Effect of soda, kraft and organosolv on *p*-NP glucuronidation by *in vivo* treatment in RKM. Rats were treated with 0, 40 and 400 mg kg⁻¹ of soda, kraft and organosolv oil palm EFB lignin for 14 121

days before sacrifice. Each bar represents the mean percentage activity relative to control \pm SD for five replicates (n=5). Statistical analysis was conducted using one-way ANOVA followed by Dunnet's test. * indicates significant difference from control (received co-solvent) ($p < 0.05$).

- Figure 4.25 HPLC analysis of 4-MU glucuronidation in RLM and RKM. The method of sample preparation and the HPLC conditions are describe in Section 3.12.1 until 3.12.11. A) blank sample from RLM. The peak at 11.125 minute in A is 4-MU, B) incubation sample from RLM. The peak at 7.017 minute in B is 4-MUG and the peak at 11.142 minute is 4-MU, C) blank sample from RKM. The peak at 10.925 minute in C is 4-MU, D) incubation sample from RKM. The peak at 7.553 minute in D is 4-MUG and the peak at 11.125 minute is 4-MU 126
- Figure 4.26 The effect of incubation time on 4-MU glucuronide formation in RLM and RKM. Reactions were performed in the presence of 4-MU (0.1 mM) and RLM or RKM (0.25 mg mL⁻¹) in a total volume incubation of 0.25 mL at 37 °C. Each point represents the mean 4-MU glucuronidated (4-MUG) (μ M) values \pm SD for triplicates (n=3). 127
- Figure 4.27 The effect of RLM and RKM protein concentration on 4-MU glucuronide formation in RLM and RKM. Reactions were performed in the presence of 4-MU (0.1 mM) and RLM or RKM (0 to 1 mg mL⁻¹) in a total volume incubation of 0.25 mL for 15 minutes at 37 °C. Each point represents the mean 4-MU glucuronidated (4-MUG) (μ M) values \pm SD for triplicates measurement (n=3). 128
- Figure 4.28 The effect of Triton X-100 concentration on 4-MU glucuronide formation in RLM and RKM. Reactions were performed in the presence of 4-MU (0.1 mM), RLM or RKM (0.125 mg mL⁻¹) in a total volume incubation of 0.25 mL for 15 minutes at 37 °C. Each point represents the mean 4-MU glucuronidated (4-MUG) (μ M) values \pm SD for triplicates (n=3). 129
- Figure 4.29 Michaelis-Menten plot for 4-MU glucuronidation in RLM and RKM, respectively. Each reaction (0.25 mL) was performed in the presence of RLM or RKM (0.125 mg mL⁻¹) and 4-MU concentration range from 0.05 – 4.0 mM. Each point represents 130

the mean of nmol per minute per milligram of 4-MU glucuronide formed \pm SD of three replicates (n=3).

- Figure 4.30 Effect of DMSO on 4-MU glucuronidation in RLM and RKM. 132
The reaction was performed in the presence of 4-MU (0.1 mM), RLM or RKM (0.125 mg mL⁻¹) at five different concentrations of DMSO. Each bar represents the mean percentage activity relative to control \pm SD for five replicates (n=5). Statistical analysis was conducted using one-way ANOVA followed by Dunnet's test. * indicates significant difference from control (without DMSO) (p < 0.05).
- Figure 4.31 Effect of soda, kraft and organosolv on 4-MU glucuronidation in RLM. 131
The reaction was performed in the presence of 4-MU (0.1 mM), RLM (0.125 mg mL⁻¹) at six different concentrations (0.01, 0.1, 1.0, 10, 100 and 500 μ g mL⁻¹) of oil palm EFB lignin. Each bar represents the mean percentage activity relative to control \pm SD for three replicates (n=3). Statistical analysis was conducted using one-way ANOVA followed by Dunnet's test. * indicates significant difference from control (without inhibitor) (p < 0.05).
- Figure 4.32 Inhibition of 4-MU glucuronidation in RLM by soda, kraft and organosolv oil palm EFB lignin compared to positive inhibitor (diclofenac). 134
Data are expressed as the mean percentage activity relative to negative control \pm SD for three replicates (n=3). Error bars represent two-sided standard error of the mean. Data points were fitted to IC₅₀ equation as described under Materials and Methods. Goodness of fit R² values were greater than 0.9.
- Figure 4.33 Effect of soda, kraft and organosolv on 4-MU glucuronidation in RKM. 135
The reaction was performed in the presence of 4-MU (0.1 mM), RKM (0.125 mg mL⁻¹) at five different concentrations (0.01, 0.1, 1.0, 10 and 100 μ g mL⁻¹) of oil palm EFB lignin. Each bar represents the mean percentage activity relative to control \pm SD for three replicates (n=3). Statistical analysis was conducted using one-way ANOVA followed by Dunnet's test. * indicates significant difference from control (without inhibitor) (p < 0.05).
- Figure 4.34 Inhibition of 4-MU glucuronidation in RKM by soda, kraft and organosolv oil palm EFB lignin compared to positive inhibitor (diclofenac). 135
Data are expressed as the mean percentage activity relative to negative control \pm SD for three replicates (n=3). Error bars represent two-sided standard error of the mean. Data points

were fitted to IC_{50} equation as described under Materials and Methods. Goodness of fit R^2 values were greater than 0.9.

- Figure 4.35 Effect of vanillin, syringaldehyde and *p*-hydroxybenzaldehyde on 4-MU glucuronidation in RLM. The reaction was performed in the presence of 4-MU (0.1 mM), RLM (0.125 mg mL⁻¹) at six different concentrations (0.01, 0.1, 1.0, 10, 100 and 500 μ M) of compounds. Each bar represents the mean percentage activity relative to control \pm SD for three replicates (n=3). Statistical analysis was conducted using one-way ANOVA followed by Dunnet's test. * indicates significant difference from control (without inhibitor) ($p < 0.05$). 137
- Figure 4.36 Effect of vanillin, syringaldehyde and *p*-hydroxybenzaldehyde on 4-MU glucuronidation in RKM. The reaction was performed in the presence of 4-MU (0.1 mM), RKM (0.125 mg mL⁻¹) at five different concentrations (0.01, 0.1, 1.0, 10, 100 and 500 μ M) of compounds. Each bar represents the mean percentage activity relative to control \pm SD for three replicates (n=3). Statistical analysis was conducted using one-way ANOVA followed by Dunnet's test. * indicates significant difference from control (without inhibitor) ($p < 0.05$). 138
- Figure 4.37 Inhibition of 4-MU glucuronidation in RLM by vanillin and syringaldehyde compared to positive inhibitor (diclofenac). Data are expressed as the mean percentage activity relative to negative control \pm SD for three replicates (n=3). Error bars represent two-sided standard error of the mean. Data points were fitted to IC_{50} equation as described under Materials and Methods. Goodness of fit R^2 values were greater than 0.9. 139
- Figure 4.38 Inhibition of 4-MU glucuronidation in RKM by vanillin and syringaldehyde compared to positive inhibitor (diclofenac). Data are expressed as the mean percentage activity relative to negative control \pm SD for three replicates (n=3). Error bars represent two-sided standard error of the mean. Data points were fitted to IC_{50} equation as described under Materials and Methods. Goodness of fit R^2 values were greater than 0.9. 140
- Figure 4.39 Lineweaver-Burk plots of inhibition of UGT-catalyzed 4-MU glucuronidation by soda oil palm EFB lignin. Data are expressed as the mean to control \pm SD for three replicates (n=3). Error bars represent two-sided standard error of the mean. Goodness of fit R^2 values were greater than 0.9. 143

- Figure 4.40 Secondary plots of UGT activity using the slopes of the primary Lineweaver-Burk plots versus the concentrations of soda oil palm EFB lignin. Each data point represents an average \pm SD of triplicates (n=3). Error bars represent two-sided standard error of the mean. Goodness of fit R^2 values were greater than 0.990. 144
- Figure 4.41 Effect of soda, kraft and organosolv on 4-MU glucuronidation by *in vivo* treatment in RLM. Rats were treated with 0, 40 and 400 mg kg⁻¹ of soda, kraft and organosolv oil palm EFB lignin for 14 days before sacrifice. Each bar represents the mean percentage activity relative to control \pm SD for three replicates (n=3). Statistical analysis was conducted using one-way ANOVA followed by Dunnet's test. * indicates significant difference from control (received co-solvent) (p < 0.05). 147
- Figure 4.42 Effect of soda, kraft and organosolv on 4-MU glucuronidation by *in vivo* treatment in RKM. Rats were treated with 0, 40 and 400 mg kg⁻¹ of soda, kraft and organosolv oil palm EFB lignin for 14 days before sacrifice. Each bar represents the mean percentage activity relative to control \pm SD for three replicates (n=3). Statistical analysis was conducted using one-way ANOVA followed by Dunnet's test. * indicates significant difference from control (received co-solvent) (p < 0.05). 148
- Figure 4.43 Michaelis-Menten kinetics plots for 4-MU glucuronidation in RLM treated with 400 mg kg⁻¹ of oil palm EFB lignin compared to control (received co-solvent). The glucuronidation rates represent the mean of three replicates (n=3) with vertical error bars indicating two sided standard error of the mean. Goodness of fit R^2 values were greater than 0.9. 153
- Figure 4.44 Michaelis-Menten kinetics plots for 4-MU glucuronidation in RKM treated with 400 mg kg⁻¹ of oil palm EFB lignin compared to control (received co-solvent). The glucuronidation rates represent the mean of three replicates (n=3) with vertical error bars indicating two sided standard error of the mean. Goodness of fit R^2 values were greater than 0.9. 154
- Figure 4.45 Optimization of incubation time. The conjugation reaction of 1-chloro-dinitrobenzene (CDNB) catalyzed by GST enzyme in RLC and RKC was performed in the total incubation volume of 300 μ L 157

in the presence of 1-chloro-dinitrobenzene (CDNB) (1mM) as a substrate for GST enzyme and the rat liver cytosolic fraction (RLC) or rat kidney cytosolic fraction (RKC) (0.125 mg mL^{-1}) for 0 – 5 minutes reaction time. Each point represents the absorbance of dinitrobenzene-glutathione conjugate formed in various time incubation \pm SD for five replicates (n=5).

- Figure 4.46 Optimization of protein concentration. The conjugation reaction of 1-chloro-dinitrobenzene (CDNB) catalyzed by GST enzyme in RLC and RKC was performed in the total incubation volume of 300 μL in the presence of 1-chloro-dinitrobenzene (CDNB) (1mM) as a substrate for GST enzyme and the rat liver cytosolic fraction (RLC) or rat kidney cytosolic fraction (RKC) ($0.0625 - 1.0 \text{ mg mL}^{-1}$) for 5 minutes reaction time. Each point represents the absorbance of dinitrobenzene-glutathione conjugate formed in various time incubation \pm SD for five replicates (n=5). 157
- Figure 4.47 Michaelis-Menten plot for dinitrobenzene-glutathione conjugate formation in RLC and RKC, respectively. Each reaction (0.3 mL) was performed in the presence of RLC or RKC (0.125 mg mL^{-1}) and CDNB concentration range from 0.01 – 20 mM. Each point represents the mean of $\mu\text{mol per minute per milligram}$ of dinitrobenzene-glutathione conjugate formed \pm SD of five replicates (n=5). 159
- Figure 4.48 Effect of DMSO on GST enzyme activity in RLC and RKC. The reaction was performed in the presence of CDNB (1.0 mM), RLC or RKC (0.125 mg mL^{-1}) at five different concentrations of DMSO. Each bar represents the mean percentage activity relative to control \pm SD for five replicates (n=5). Statistical analysis was conducted using one-way ANOVA followed by Dunnet's test. * indicates significant difference from control (without DMSO) ($p < 0.05$). 160
- Figure 4.49 Effect of soda, kraft and organosolv oil palm EFB lignin on GST enzyme activity in RLC. The reaction was performed in the presence of CDNB (1.0 mM), RLC (0.125 mg mL^{-1}) at six different concentrations (0.01, 0.1, 1.0, 10, 50 and $100 \mu\text{g mL}^{-1}$) of oil palm EFB lignin. Each bar represents the mean percentage activity relative to control \pm SD for five replicates (n=5). Statistical analysis was conducted using one-way ANOVA followed by Dunnet's test. * indicates significant difference from 161

control (without inhibitor) ($p < 0.05$).

- Figure 4.50 Inhibitory effect of soda, kraft and organosolv compare to positive inhibitor (tannic acid) on CDNB conjugation reaction catalyzed by the GST enzyme from RLC. Concentration of inhibitors ranged from 0.01 – 100 $\mu\text{g mL}^{-1}$. Data are expressed as the mean percentage activity relative to negative control \pm SD for five replicates ($n=5$). Error bars represent two-sided standard error of the mean. Data points were fitted to IC_{50} equation as described under Materials and Methods. Goodness of fit R^2 values were greater than 0.9. 162
- Figure 4.51 Effect of soda, kraft and organosolv oil palm EFB lignin on GST enzyme activity in RKC. The reaction was performed in the presence of CDNB (1.0 mM), RKC (0.125 mg mL^{-1}) at six different concentrations (0.01, 0.1, 1.0, 10, 50 and 100 $\mu\text{g mL}^{-1}$) of oil palm EFB lignin. Each bar represents the mean percentage activity relative to control \pm SD for five replicates ($n=5$). Statistical analysis was conducted using one-way ANOVA followed by Dunnet's test. * indicates significant difference from control (without inhibitor) ($p < 0.05$). 164
- Figure 4.52 Inhibitory effect of soda, kraft and organosolv compare to positive inhibitor (tannic acid) on CDNB conjugation reaction catalyzed by the GST enzyme from RKC. Concentration of inhibitors ranged from 0.01 – 100 $\mu\text{g mL}^{-1}$. Data are expressed as the mean percentage activity relative to negative control \pm SD for five replicates ($n=5$). Error bars represent two-sided standard error of the mean. Data points were fitted to IC_{50} equation as described under Materials and Methods. Goodness of fit R^2 values were greater than 0.9. 165
- Figure 4.53 Effect of vanillin, syringaldehyde and *p*-hydroxybenzaldehyde on GST enzyme activity in RLC. The reaction was performed in the presence of CDNB (1.0 mM), RLC (0.125 mg mL^{-1}) at six different concentrations (0.01, 0.1, 1.0, 10, 50 and 100 μM) of compounds. Each bar represents the mean percentage activity relative to control \pm SD for five replicates ($n=5$). Statistical analysis was conducted using one-way ANOVA followed by Dunnet's test. * indicates significant difference from control (without inhibitor) ($p < 0.05$). 168
- Figure 4.54 Effect of vanillin, syringaldehyde and *p*-hydroxybenzaldehyde on GST enzyme activity in RKC. The reaction was performed in the 169

presence of CDNB (1.0 mM), RKC (0.125 mg mL⁻¹) at six different concentrations (0.01, 0.1, 1.0, 10, 50 and 100 μM) of compounds. Each bar represents the mean percentage activity relative to control ± SD for five replicates (n=5). Statistical analysis was conducted using one-way ANOVA followed by Dunnet's test. * indicates significant difference from control (without inhibitor) (p < 0.05).

- Figure 4.55 Effect of soda, kraft and organosolv on GST enzyme activity by *in vivo* treatment in RLC. Rats were treated with 0, 40 and 400 mg kg⁻¹ of soda, kraft and organosolv oil palm EFB lignin for 14 days before sacrifice. Each bar represents the mean percentage activity relative to control ± SD for five replicates (n=5). Statistical analysis was conducted using one-way ANOVA followed by Dunnet's test. * indicates significant difference from control (received co-solvent) (p < 0.05). 173
- Figure 4.56 Effect of soda, kraft and organosolv on GST enzyme activity by *in vivo* treatment in RKC. Rats were treated with 0, 40 and 400 mg kg⁻¹ of soda, kraft and organosolv oil palm EFB lignin for 14 days before sacrifice. Each bar represents the mean percentage activity relative to control ± SD for five replicates (n=5). Statistical analysis was conducted using one-way ANOVA followed by Dunnet's test. * indicates significant difference from control (received co-solvent) (p < 0.05). 175

LIST OF SYMBOLS

%	Percentage
°C	Degree celcius
μ	Micro
μg mL ⁻¹	Microgram per milliliter
μg	Microgram
μg mL ⁻¹	Microgram per milliliter
μL	Microliter
μM	Micromolar
μm	Micrometer
cm	Centimeter
g	Grams
mg mL ⁻¹	Milligrams per milliliter
mM	Milimolar
mmol g ⁻¹	milimole per gram
R ²	Coefficient of determination
v/v	Volume over volume
w/v	Weight over volume

LIST OF ABBREVIATIONS

^{13}C NMR	Carbon-13 NMR spectroscopy
^{31}P NMR	Phosphorus-31 NMR spectroscopy
4-MU	4-methylumbelliferone
4-MUG	4-methylumbelliferone glucuronide
<i>Ad libitum</i>	To be taken as wanted
AlCl_3	Aluminium chloride
ANOVA	Analysis of variance
BSA	Bovine serum albumin
CDNB	1-chloro-2,4-dinitrobenzene
CL_{int}	Intrinsic clearance
$\text{CuSO}_4 \cdot 5\text{H}_2\text{O}$	Copper (II) sulfat pentahydrate
CYP	Cytochrome P450
DMSO	Dimethyl sulfoxide
DPPH	2,2-diphenyl-1-picryl-hydrazyl
EFB	Empty fruit bunch
FDA	Food and Drug Administration
FT-IR	Fourier Transform Infrared
GC-MS	Gas chromatography–mass spectrometry
GIT	Gastrointestinal tract
GLC	Gas liquid chromatography
GPC	Gel permeation chromatography
GSH	Glutathione
GST	Glutathione S-transferase
HPLC	High performance liquid chromatography
IC_{50}	Half maximal inhibitory concentration
KCl	Potassium chloride
K_i	Dissociation constant of an inhibitor enzyme complex
K_m	Michaelis-Menten constant
mg GAE/g	Milligram gallic acid equivalents in 1 gram of sample
mg QAE/g	Milligram quercetin equivalence in 1 gram of sample

MgCl ₂	Magnesium chloride
min	Minutes
M _n	Number average molecular weight
M _w	Weight average molecular weight
M _w /M _n	Polydispersity
MAPEG	Membrane-Associated Proteins in Eicosanoid and Glutathione metabolism
Na ₂ CO ₃	Sodium carbonate
NaCl	Sodium chloride
NaK Tartrate	Sodium potassium tartrate
NaNO ₂	Sodium nitrite
NaOH	Sodium hydroxide
nmol	Nanomole
<i>p</i> -NP	<i>para</i> -Nitrophenol
<i>p</i> -NPG	<i>para</i> -Nitrophenol glucuronide
QE	Quercetin equivalent
RKM	Rat kidney microsomes
RKC	Rat kidney cytosolic fraction
RLC	Rat liver cytosolic fraction
RLM	Rat liver microsome
rpm	Revolution per minute
RSD	Relative standard deviation
RT-PCR	Reverse transcription polymerase chain reaction
SD	Standard deviation
TCA	Trichloroacetic acid
TMDP	2-chloro-4,4,5,5-tetramethyl-1,2,3-dioxaphospholane
Tris-HCl	Tris(hydroxymethyl)aminomethane hydrochloride
UDPGA	Uridine 5'-diphospho-glucuronic acid
UGT	Uridine 5'-diphospho-glucuronosyltransferases
UV	Ultraviolet
V _{max}	Maximal reaction velocity

LIST OF APPENDICES

	Page	
Appendix A	Animal ethical clearance letter	207
Appendix B	Standard curve of pure compounds A: hydroxybenzoic acid, B: vanillic acid, C: syringic acid, D: <i>p</i> -hydroxybenzaldehyde, E: vanillin, F: <i>p</i> -coumaric acid, G: syringaldehyde and H: ferulic acid to determine the yield (% dry sample, w/w) of compounds from alkaline nitrobenzene oxidation of oil palm EFB lignin	208
Appendix C	One of the standard curves of bovine serum albumin (BSA) for protein determination in rat liver microsome (RLM) and rat kidney microsome (RKM). Each point represents the mean absorbance values \pm SD for triplicates measurement (n=3)	211
Appendix D	One of the standard curves of <i>p</i> -nitrophenol (<i>p</i> -NP). Each point represents the mean absorbance values \pm SD for triplicates measurement (n=3)	212
Appendix E	One of the calibration curves of 4-methylumbelliferone glucuronide (4-MUG). Each point represents the mean peak area of 4-MUG \pm SD for triplicates measurement (n=3)	213
Appendix F	One of the standard curves of bovine serum albumin (BSA) for protein determination in rat liver cytosolic fraction (RLC) and rat kidney cytosolic fraction (RKC). Each point represents the mean absorbance values \pm SD for triplicates measurement (n=3)	214

**PENILAIAN TERHADAP LIGNIN TANDAN KOSONG KELAPA SAWIT
PADA METABOLISME DRUG FASA II YANG TERPILIH**

ABSTRAK

Dalam usaha untuk membangunkan lignin tandan kosong kelapa sawit (TKKS) sebagai makanan tambahan dalam nutraseutikal dan kesihatan, penyelidikan tentang potensinya dalam berinteraksi dengan drug lain melalui perencatan atau peningkatan enzim metabolisme drug (DME) mampu memastikan keselamatan produk. Oleh itu, kajian ini dijalankan untuk mengkaji kesan lignin TKKS dan sebatian-sebatian teroksida utamanya terhadap DME fasa II UDP-glukuronosiltransferase (UGT) dalam mikrosom hati tikus (RLM) dan mikrosom ginjal tikus (RKM) serta glutathion S-transferase (GST) dalam fraksi sitosol hati tikus (RLC) dan fraksi sitosol ginjal tikus (RKC) secara rawatan *in vitro* dan *in vivo*. Pencirian lignin TKKS menunjukkan bahawa ketiga-tiga jenis ekstrak lignin TKKS (soda, kraft dan organosolv) terdiri daripada siringil dan guaiasil. Jumlah kandungan flavonoid pada lignin TKKS meningkat dalam turutan organosolv < kraft < soda. Analisis kromatografi cecair berprestasi tinggi (HPLC) menunjukkan bahawa siringaldehid merupakan sebatian teroksida utama yang terdapat dalam lignin TKKS diikuti dengan vanilin dan *p*-hidroksibenzaldehid. Lignin TKKS dinilai sebagai aktiviti penghapus radikal bebas DPPH yang berpotensi. Keputusan kajian menunjukkan lignin dengan kandungan kumpulan fenolik (ArOH) yang tinggi, jisim molar (M_w) yang rendah dan poliserakan (M_w/M_n) yang kecil menunjukkan aktiviti penghapus radikal bebas DPPH yang tinggi. *p*-nitrofenol (*p*-NP) dan 4-metilumbelliferon (4-MU) masing-masing digunakan sebagai substrat prob dalam asai UGT, manakala 1-kloro-2,4-dinitrobenzena (CDNB) digunakan sebagai substrat prob dalam asai GST.

Bagi perawatan *in vitro*, potensi perencatan lignin TKKS bagi kedua-dua glukuronidasi *p*-NP dan 4-MU dalam RLM dan RKM dipengaruhi oleh kandungan flavonoidnya (soda > kraft > organosolv). Potensi perencatan juga dipengaruhi oleh kehadiran vanilin dalam ekstrak lignin. Bagi aktiviti enzim GST, potensi perencatan lignin TKKS dalam RLC dan RKC juga dipengaruhi oleh kandungan flavonoidnya (soda > kraft > organosolv). Walau bagaimanapun, potensi perencatan lignin TKKS terhadap aktiviti enzim GST dalam kedua-dua RLC dan RKC tidak dipengaruhi oleh sebatian-sebatian teroksida utamanya. Bagi rawatan *in vivo*, dos rendah (40 mg kg⁻¹) lignin TKKS mengurangkan glukuronidasi *p*-NP dan 4-MU dalam kedua-dua RLM dan RKM. Manakala, dos tinggi (400 mg kg⁻¹) lignin TKKS meningkatkan glukuronidasi *p*-NP dan 4-MU dalam kedua-dua RLM dan RKM. Bagi aktiviti enzim GST dalam RLC dan RKC, kedua-dua dos meningkatkan aktiviti enzim. Keputusan juga menunjukkan kandungan flavonoid lignin TKKS berkemungkinan bertanggungjawab terhadap peningkatan aktiviti GST yang diperhatikan. Kesimpulannya, kajian ini mencadangkan lignin TKKS boleh memberi kesan terhadap konjugasi substrat oleh enzim yang melibatkan enzim UGT1A6 dan enzim GST kelas μ - terutamanya dalam hati tikus.

AN EVALUATION OF OIL PALM EMPTY FRUIT BUNCH LIGNIN ON SELECTED PHASE II DRUG METABOLIZING ENZYMES

ABSTRACT

In order to develop oil palm empty fruit bunch (EFB) lignin as a nutraceutical and health supplement, the investigation of its potential in interacting with other drugs via inhibition or induction of drug metabolizing enzymes (DME) would contribute towards product safety. Therefore, this study was carried out to investigate the effect of oil palm EFB lignin and its main oxidative compounds on phase II DME, UDP-glucuronosyltransferases (UGT) in rat liver microsomes (RLM) and rat kidney microsomes (RKM) as well as glutathione-S-transferases (GST) in rat liver cytosolic fraction (RLC) and rat kidney cytosolic fraction (RKC) by *in vitro* and *in vivo* treatment. The characterization of oil palm EFB lignin showed that all three types of oil palm EFB lignin extracts (soda, kraft and organosolv) consist of syringyl and guaiacyl. The total flavonoids content of oil palm EFB lignin was increased in the order of organosolv < kraft < soda. The high performance liquid chromatography (HPLC) analysis revealed that syringaldehyde was the main oxidation compound in oil palm EFB lignin followed by vanillin and *p*-hydroxybenzaldehyde. The oil palm EFB lignin evaluated as potential DPPH-radical scavenging activity. Results indicated that the lignin with more phenolic group (ArOH) content, low molecular weight (M_w) and narrow polydispersity (M_w/M_n) showed high DPPH-radical scavenging activity. *p*-nitrophenol (*p*-NP) and 4-methylumbelliferone (4-MU) were employed as probe substrates in UGT assays, respectively, while 1-chloro-2,4-dinitrobenzene (CDNB) was employed as probe substrate in GST assay. For *in vitro* treatment, the inhibitory potency of oil palm EFB lignin for both *p*-NP and 4-MU

glucuronidation in RLM and RKM were encouraged by its flavonoids content (soda > kraft > organosolv). The inhibitory potency was also encouraged by the presence of vanillin in the lignin extracts. For GST activity, the inhibitory potency of oil palm EFB lignin in RLC and RKC also encouraged by its flavonoids content (soda > kraft > organosolv). However, the inhibitory potency of oil palm EFB lignin on GST activity in both RLC and RKC was not encouraged by its main oxidation compounds. For *in vivo* treatment, the lower dosage (40 mg kg⁻¹) of oil palm EFB lignin decreased the *p*-NP and 4-MU glucuronidation in both RLM and RKM. However, higher dosage (400 mg kg⁻¹) of oil palm EFB lignin increased the *p*-NP and 4-MU glucuronidation in both RLM and RKM. For GST activity in RLC and RKC, both dosages increased the enzyme activity. Result also indicated that flavonoids content of oil palm EFB lignin might be responsible for the observed induction in GST activity. In conclusion, the findings suggest that oil palm EFB lignin may affect the conjugation of substrates by phase II enzymes which involved UGT1A6 and GST class μ - particularly in rat liver.

CHAPTER 1

INTRODUCTION

1.1 Background of the study

Oil palm empty fruit bunch (EFB) lignin is known to be a good feedstock to produce biomaterial such as activated carbon (Fierro et al., 2006), fibre board (Velásquez et al., 2003), adhesives (Danielson and Simonson, 1998; Kouisni et al., 2011), adsorbent (Mohamad Ibrahim et al., 2010a), bio-corrosion inhibitors (Akbarzadeh et al., 2011) and as filler in the formulation of inks, varnishes and paints (Belgacem et al., 2003). Besides, lignin which is extracted from lignocellulosic waste such as oil palm empty fruit bunch (EFB), sugar cane and wood has potential application in pharmaceutical and food product such as emulsifier (Mohamad Ibrahim 2010), antidiarrheal drug (Mitjans et al., 2001) and natural antioxidant (Dizhbite et al., 2004; Mitjans and Vinardell, 2005; Pan et al., 2006; Ugartondo et al., 2008).

Therefore, the various application of oil palm EFB lignin especially in pharmaceuticals and food products area give additional value to lignin. Usually, public believe that natural product can be equated to be safe. For this reason, they often self-prescribed without knowing its potentially dangerous implications. For example, the potential of the metabolic effect of herbals and phytochemicals on the efficacy and/or toxicity of drug, which is commonly referred to as herb-drug interactions, which may lead to poor clinical outcomes, is one of the issues of concern to clinicians (Gardiner et al., 2008). The consequence of herb-drug

interactions can be beneficial effects such as cancer prevention, undesirable effects such as pharmacokinetics interactions with co-administered drugs and harmful effects; such as organ toxicity or carcinogenesis (Mandlekar et al., 2006).

Since the development of the application of oil palm EFB lignin in pharmaceuticals and food products is growing nowadays, attention must also be given to the investigation of the effects of oil palm EFB lignin on the most important conjugative enzymes of phase II metabolism (UGT and GST). These enzymes mostly exhibit broad substrate selectivity and eliminate many therapeutic drugs, endogenous compounds and secondary plant metabolites such as flavonoids and polyphenolic compounds. In addition, the investigation of potential drug interaction with oil palm EFB lignin through competition with drugs for this conjugation pathway is needed to ensure consumer safety (Mohamed and Frye, 2011).

The metabolism of xenobiotic (foreign compounds) and endogenous (internal compounds) is the body's own detoxifying system which is crucial for its survival. Generally DMEs eliminate xenobiotics and endogenous substances by increasing solubility through the functionalization process in phase I and/or conjugation reactions in phase II. Phase I reactions involve oxidation, reduction and hydrolysis, where a functional group is exposed or introduced, usually resulting in a small increase in xenobiotic hydrophilicity and further prepare the xenobiotics for phase II (Gibson and Skett, 2001; Nassar, 2009). Phase II reactions involve conjugation reactions including conjugation with glutathione and other amino acids, glucuronidation, sulfation, acetylation and/or methylation. Therefore, phase II is the true 'detoxification' of both endogenous and foreign compounds to produce metabolites that are generally water-soluble and easily excreted.

Glucuronidation reaction involves conjugation of suitable functional groups on a substrate with glucuronic acid. This reaction, which requires UDP-glucuronic acid (UDPGA) as a co-factor, is catalyzed by the enzyme UDP-glucuronosyltransferase (UGT). It is responsible for the elimination of structurally diverse xenobiotics and endogenous compounds (Miners and Mackenzie, 1991; Radomska-Pandya et al., 1999; Tukey and Strassburg, 2000). Glucuronidation serves as an elimination pathway in humans for numerous dietary chemicals, environmental pollution and endogenous compound such as bilirubin, bile acids and hydroxysteroid. Moreover, glucuronidation facilitates excretion of these compounds and the parent compounds in urine and bile as their hydrophilic conjugates and generally results in detoxification although a limited number of glucuronides possess biological activity (Ritter, 2000). In particular, glucuronidation is an essential clearance mechanism for drugs from all therapeutic classes.

Another major phase II detoxification enzyme which is involved in the metabolism of xenobiotics and plays an important role in cellular protection against oxidative stress is glutathione S-transferase (GST) enzymes. GST plays a major role in the detoxification of epoxides derived from polycyclic aromatic hydrocarbons (PAHs) and alpha-beta unsaturated ketones. Moreover, a number of endogenous compounds such as prostaglandins and steroids are metabolized via glutathione conjugation (van Bladeren, 2000). The major biological function of glutathione transferase appears to be defence against reactive and toxic electrophiles such as reactive oxygen species (superoxide radical and hydrogen peroxide) that arise through normal metabolic processes.

Therefore, this study was carried out to determine the effect of oil palm EFB lignin (soda, kraft and organosolv) and its main oxidative compounds (vanillin,

syringaldehyde and *p*-hydroxybenzaldehyde) on UGT and GST activity by *in vitro* and *in vivo* treatment. Rat liver microsomes (RLM) and rat kidney microsomes (RKM) were used as sources of the UGT enzyme, while rat liver cytosolic fraction (RLC) and rat kidneys cytosolic fraction (RKC) were used as the sources for GST enzymes. For UGT enzyme assay, *para*-nitrophenol (*p*-NP) and 4-methylumbelliferone (4-MU) were used as substrates while 1-chloro-2,4-dinitrobenzene (CDNB) was used as substrate for GST enzyme assay. Spectrophotometry and high performance liquid chromatography (HPLC) were the analytical methods used to evaluate the activities of the enzymes studied.

1.2 Problem statement

The development of oil palm EFB lignin for its application in pharmaceuticals and food industries promises an additional value to lignin. However, before oil palm EFB lignin can be developed as a nutraceutical and health supplement, the investigation of its potential in interacting with other drugs or pharmaceutical agents must be carry out to ensure product safety. This is because the oil palm EFB lignin would be metabolized by the same drug metabolism enzymes (DMEs) as other drugs or pharmaceutical agents. Therefore, it could results in food-drug interaction and may cause adverse side effects (Honig et al., 1993; Sorensen, 2002; Brandin et al., 2007). As an example, the inhibitory effect of drug metabolizing enzymes can cause harmful side effects such as increased plasma level and prolonged pharmacological effects of the parent drug and enhancement of drug induced toxicity (Hernandez and Rathinavelu, 2006; Gardiner et al., 2008).

Given the importance of glucuronidation and glutathione conjugation as a detoxification and metabolic pathway for numerous xenobiotics and endogenous

compounds and the development of oil palm EFB lignin for pharmaceuticals and food industries applications, there is growing interest in the study of the potential for its interaction effect on phase II drug metabolism enzymes activity. In addition, the investigation of potential drug interaction with oil palm EFB lignin of drug metabolizing enzymes for this conjugation pathway is needed to ensure consumer safety. Therefore, to overcome the above problems, the aims of this study are:

- 1) To characterize the oil palm EFB lignin extract of soda, kraft and organosolv via colorimetric (flavonoids content), chromatographic (gel permeation chromatography and high performance liquid chromatography) and spectroscopic (nuclear magnetic resonance) methods.
- 2) To determine the correlation between 2,2-diphenyl-1-picrylhydrazyl (DPPH) radical scavenging activity of oil palm EFB lignin and its phenolic content, flavonoids content and molecular weight.
- 3) To investigate the effect of oil palm EFB lignin extract of soda, kraft and organosolv and its main oxidative compounds (vanillin, syringaldehyde and *p*-hydroxybenzaldehyde) on UDP-glucuronosyltransferase (UGT) enzyme activity by *in vitro* and *in vivo* (sub-chronic) treatment using *p*-nitrophenol (*p*-NP) and 4-methylumbelliferone (4-MU), respectively as probe substrates in rat liver and kidney microsomes. Effect on *p*-NP is done using spectrophotometry method, while effect on 4-MU employed high performance liquid chromatography (HPLC) method.
- 4) To evaluate the effect of oil palm EFB lignin extract of soda, kraft and organosolv and its main oxidative compounds (vanillin, syringaldehyde and *p*-hydroxybenzaldehyde) on glutathione S-transferase (GST) enzyme activity

by *in vitro* and *in vivo* (sub-chronic) treatment using 1-chloro-2,4-dinitrobenzene (CDNB) as a probe substrate in rat liver and kidney cytosolic fraction, respectively.

CHAPTER 2

LITERATURE REVIEW

2.1 Oil palm empty fruit bunch

Based on the statistic shown by Malaysian Palm Oil Board (MPOB), Malaysia is second world's leading producers of palm oil after Indonesia. The cultivation of mature and immature palm trees cover a total of 5.64 million hectares representing 52 % of the total area (10.9 million hectares) designated for agriculture and 17% of overall Malaysian territory (Ministry of Plantation Industries and Commodities, 2016). Simultaneously, cultivation also generates a substantial amount of lignocellulosic agriculture wastes. As far as oil palm is concerned, Malaysia has approximately 445 palm oil mills, processing about 97.57 million tons of fresh fruit bunch and producing an estimated 56 million tons of crop residue annually in the form of empty fruit bunch (EFB), fibres, trunks, fronds and shells (Malaysian Palm Oil Board, 2016). As one of the main exporter of palm oil in the world, utilization of oil palm biomass for the production of environmental-friendly biomaterials has become an attractive approach (Chew and Bhatia, 2008). Furthermore, the development of lignocellulosic industry is predicted to be an economy booster for small scale farmers.

The oil palm empty fruit bunch (EFB) refers to a fiber residue formed after the oil palm fruits are separated from the bunches at palm oil mills using fruit shredders. The oil palm EFB is considered as non-hazardous biodegradable material as the fibres are clean, non-carcinogenic and free from pesticides and soft

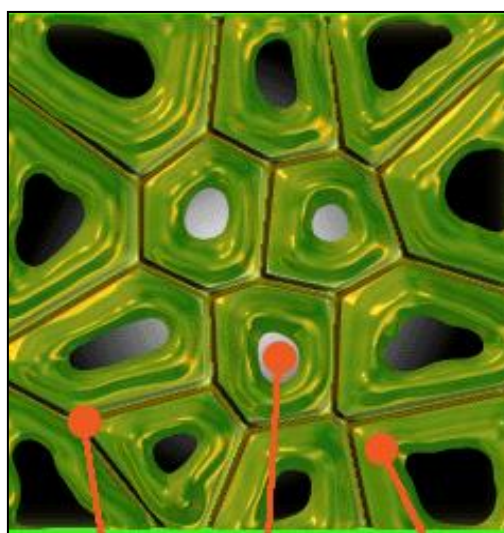
parenchyma cells (Abdullah and Sulaiman, 2013). Oil palm EFB contained polymeric component such as hemicellulose (20-21 %), cellulose (35-40 %) and lignin (17-21 %) (Mohamad Ibrahim et al., 2010b). This renewable resource (oil palm EFB) as a raw material has been investigated by many researchers such as in polymer blended composite manufacturing (Rozman et al., 2004), the cellulose production (Umi Kalsom et al., 1997) and the production of various chemicals (Rahman et al., 2007). Furthermore, continuous studies by local researches had investigated the potential of oil palm EFB as a raw material in pulp and paper manufacturing as it is high in α -cellulose content (Khoo and Lee, 1991; Wan Rosli et al., 1998). Through its potential in the future pulp and paper industry, it can decrease the deforestation rate in the country.

However the pulping process also potentially produces effluent, namely black liquor. Irresponsible plant operators would simply drain the waste into the river as a way of disposing the black liquor. This will lead to situation of river sediment and cause water pollution. Therefore, this problem could be addressed through the recycling of black liquor to obtain lignin. The pulping process is considered special because it not only produces paper but it also recycles the black liquor to obtain a new product namely lignin.

2.2 Oil palm empty fruit bunch lignin

Lignin is a major cell wall component in plants (Figure 2.1). Lignin provides support for the plant, contributes to the transport of nutrients and water and protects against microorganisms (Buranov and Mazza, 2008). Lignin is an amorphous polymer built up by oxidative coupling of three major phenylpropanoid units namely *trans-p*-coumaryl alcohol, *trans-coniferyl* alcohol and *trans-sinapyl* alcohol (Lewis

and Yamamoto, 1990). The phenylpropanoids form a randomised structure in a three-dimensional network inside the cell wall as shown in the Figure 2.2. The phenylpropane units are commonly classified into three main types which differ in the amount of methoxyl groups namely *p*-hydroxyphenyl (H), guaiacyl (G) and syringyl (S) lignin (Lewis and Yamamoto, 1990). These basic units are primarily attached to different types of aryl-aryl ether type and have more than 10 different types of linkages (Brunow et al., 1999).



Lignin Lumen Fibre

Figure 2.1: Lignin position in vascular plant (Lewis and Yamamoto, 1990)

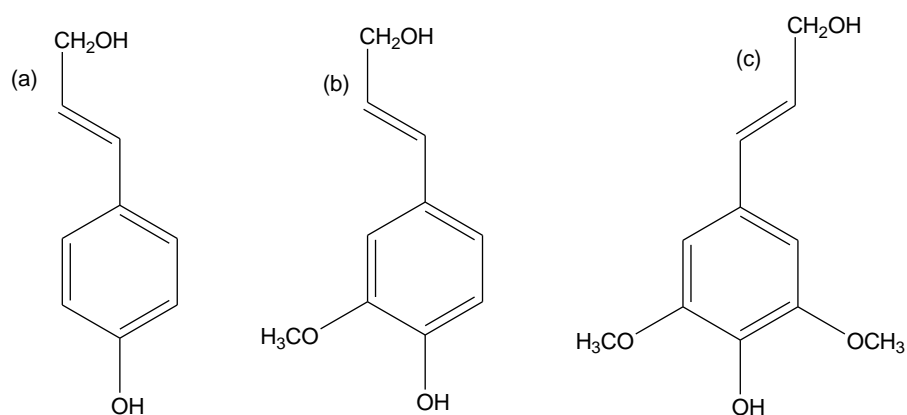


Figure 2.2: Lignin consist of three major phenylpropanoid units which are (a) *trans-p*-coumaryl alcohol, (b) *trans-coniferyl* alcohol and (c) *trans-sinapyl* alcohol (Lewis and Yamamoto)

Oil palm empty fruit bunch (EFB) lignin is obtained from the pulping process of EFB. Generally, this process is accomplished by the digestion of EFB with sodium hydroxide (NaOH) for 3 hours at a pressure of 10 bars to separate the pulp and black liquor. The pulp can be processed into paper while the black liquor will be extracted with organic acid such as sulphuric acid (H_2SO_4) to obtain a precipitate. The precipitate will be filtered and the dried residue obtained will be the lignin (Wan Rosli et al., 1998). Figure 2.3 summarized the paper making process and lignin from EFB. Through the papermaking process, the EFB is used as a raw material, while the toxic waste namely, black liquor can be recycled to obtain lignin. There are three types of oil palm EFB lignin which were used in this study namely soda, kraft and organosolv. The different types of oil palm EFB lignin depend on the chemical and method which were used during pulping processes.

The alkaline pulping process such as soda and kraft pulping is known as potential pulping process for non-woody materials (Feng and Alén, 2001; Garcia et al., 2009). Both of these pulping processes function to liberate lignin, hemicelluloses and cellulose to enhance the quality of the pulp (Wan Rosli et al., 1998). The kraft pulping is a dominant pulping process because it enables pulping of different tree species, recovers and reuses all pulping chemicals and produces a high quality paper. Kraft lignin contains several characteristic features distinguishing it from native lignin and other technical lignins. It contains an increased amount of phenolic hydroxyl groups due to extensive cleavage of β -aryl bonds during cooking (Prinsen et al., 2013).

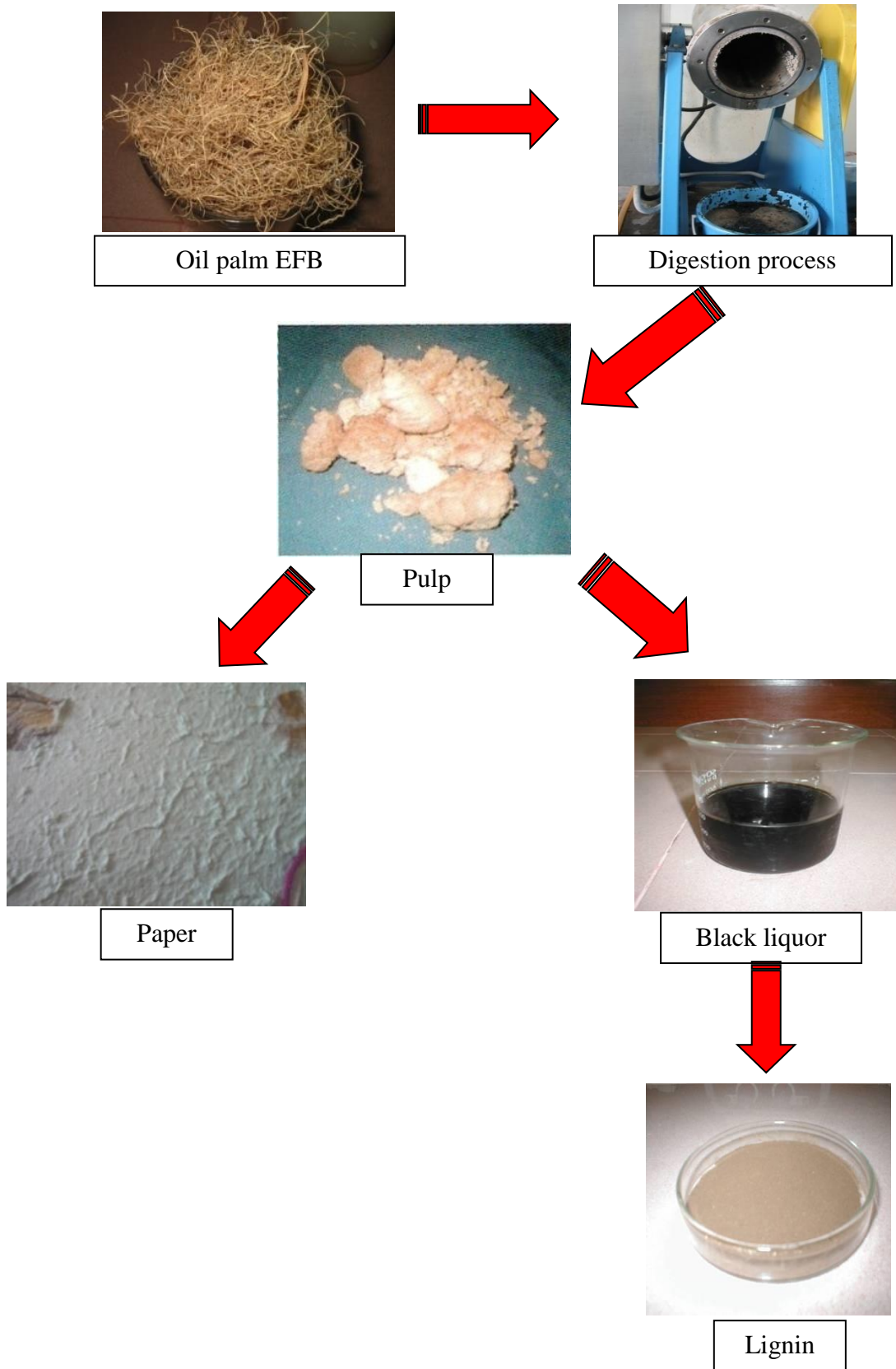


Figure 2.3: Flowchart of the production of paper and lignin from oil palm empty fruit bunch

However, there is a growing interest in applying soda pulping for non-woody based material in papermaking such as empty fruit bunch fibre (Wan Rosli et al., 2004; Wan Rosli et al., 2005). The main difference of soda pulping compared to the kraft pulping is the sulphur-free medium of the cooking liquor (Gullischsen and Fogenholm, 2000). Soda lignin is sulphur-free; therefore, its chemical composition is closer to natural lignin compare to kraft lignin (Nadif et al., 2002; Wormeyer et al., 2011).

The organic pulping process such as organosolv pulping is also one of the most promising alternatives to existing pulping technologies. Lignin is separated via solubilization from organosolv pulping process. Solubilization makes it possible to obtain a less modified lignin. The properties of organosolv lignin differ from other technical lignins. The major features are low molecular weight and high chemical purity. Organosolv lignin is hydrophobic and show very poor solubility in water (Lora and Glasser, 2002). Organosolv pulping produces lignin of high quality, containing a lot of reactive side chains available for further chemical reactions (Meister, 2002).

Organosolv lignin has been used as filler in the formulation of inks, varnishes and paints (Belgacem et al., 2003). Besides, organosolv lignin also can be used in the same applications as kraft and soda lignin. In addition, organosolv lignin could find valuable applications in the fields of adhesives, fibres, films and biodegradable polymers (Vasquez et al., 1999; Cetin and Ozmen, 2002; Pereira et al., 2007).

Kraft lignin, which is produced from kraft pulping process has been successfully converted to activated carbon (Fierro et al., 2006) and is used to produce fibreboard (Velásquez et al., 2003). Kraft lignin has also been successfully formulated as adhesives especially in the formulation of lignin-phenol-formaldehyde

resins (Danielson and Simonson, 1998; Kouisni et al., 2011). Lignin is more readily available, less toxic and less expensive than phenol. Using kraft lignin to replace phenol in the formulation of phenol-formaldehyde resin is considered a potentially attractive application from the economic and ecological point of view because the phenol price is subjected to fluctuations in oil prices and supply and is generally lower than demand.

Soda lignin which is produced from soda pulping process also has been successfully converted to biomaterial products such as adsorbent for heavy metals removal (Mohamad Ibrahim et al., 2010a), bio-corrosion inhibitors (Akbarzadeh et al., 2011). Soda lignin and phenol are structurally similar for possessing more phenolic hydroxyl groups. Therefore, soda lignin also has potential to be used as a substitute for part of the phenol in the synthesis of phenol-formaldehyde resin (Jin et al., 2010; Mohamad Ibrahim et al., 2011).

2.3 The applications of lignin for pharmaceutical and food industry

In addition to produce biomaterials products, lignin which is extracted from any lignocellulosic waste such as oil palm EFB, sugar cane, wood and others also has potential in pharmaceutical and food product industry. The application include as emulsifier (Mohamad Ibrahim, 2010), antidiarrheal drug (Mitjans et al., 2001) and natural antioxidant (Dizhbite et al., 2004; Mitjans and Vinardell, 2005; Pan et al., 2006; Ugartondo et al., 2008).

2.3.1 The potential of oil palm EFB lignin as an emulsifying agent for oil in water system emulsion

Emulsions are thermodynamically unstable system because it is a hydrophobic colloid. While the contact between oil and water molecules is

energetically unfavourable, they tend to breakdown with time (Suzanne Nielsen, 2010). There are two types of emulsion. The first type is oil-in-water (O/W) emulsion which is droplets of oil dispersed within water. This type of emulsion is applied in producing paints, detergents, ice cream and milk. The second type is water-in-oil (W/O) emulsion which is water droplets dispersed in oil. This system is widely used in food industry such as in producing of margarine, mayonnaise and cream (Mohamad Ibrahim, 2010). Since emulsion is not stable, it needs emulsifying agent or emulsifier to stabilize it by reducing the surface tensions between the oil and water phases (Suzanne Nielsen, 2010).

An emulsifier is a surface-active molecule that absorbs to the surface of an emulsion droplet to form a protective coating that prevents the droplets from aggregating with one another. An emulsifier also reduces the interfacial tension and therefore facilitates the disruption of emulsion droplets during homogenization (Suzanne Nielsen, 2010). It consists of hydrophilic parts (water soluble) and lipophilic parts (oil soluble). When emulsifier is added to a mixture of water and oil, the hydrophilic end will bond with water while the lipophilic ends will bond with oil. In this way, the oil and water stay mixed together and this means that the emulsion is being stabilized (Mohamad Ibrahim, 2010). Although lignin does not form micelles, the molecule has both hydrophilic and lipophilic moieties (Gundersen and Sjöblom, 1999). With these properties, oil palm EFB lignin can be applied as an emulsifying agent in pharmaceuticals and food product industries.

A study by Mohamad Ibrahim (2010) has shown that the optimum percentage of emulsifier (oil palm EFB lignin) in the formulation of water in oil system is 16% (v/v). The mixture was homogenized by using a Silverson Laboratory Mixer Emulsifier for 2 minutes. The same procedures were repeated for the commercial

emulsifier (egg lecithin) and the performance of each formulation was compared. This investigation proved that oil palm EFB lignin has great potential as an emulsifying agent for oil in water system emulsion compared to the commercial emulsifying agent (egg lecithin).

2.3.2 Lignin-based formulation (Ligmed-A) as antidiarrheal drug

The potential toxic effect of 4-days oral treatment with a lignin-based formulation (Ligmed-A) which is used to treat diarrhea in weaning pigs has been studied by Mitjans et al. (2001). Ligmed-A which was prepared from sugarcane, is composed of 90% lignin.

Ligmed-A has been manufactured in Cuba since the 1990s and it shows similar efficacy to other drugs used to treat diarrhea (Fragas et al., 1997). However the oral administration of this compound may affect the activity of the small intestine and may damage mucous membranes, thereby reducing nutrient absorption. The study was carried out by daily oral dose of 2 g kg^{-1} of Ligmed-A to male Wistar albino (210 g) rats for 4 days which is the recommended dose and duration of administration in pigs. This study concluded that oral administration of Ligmed-A for 4 days did not affect mucosal sucrose, alkaline phosphatase activities or the morphometry of these three segments (duodenum, jejunum and ileum) in rats. The study also indicated that Ligmed-A could provide a potent antidiarrheal treatment in the veterinary area.

2.3.3 Antioxidant properties of lignin

The antioxidant properties of natural substances as well as lignin with different origins have been of interest of many researchers in the past years

(Sakagami et al., 1992; Dizhbite et al., 2004; Mitjans and Vinardell, 2005; Pan et al., 2006; Vinardell et al., 2008). Oxygen free radicals and other reactive oxygen species can cause oxidative injury to living organisms and thus play an important role in many lifestyle-related diseases such as arthritis, atherosclerosis, emphysema and cancer (Kehrer, 1993; Jacob, 1994; Halliwell et al., 1995).

Lignin is an effective free radical scavenger because it stabilizes the reactions induced by oxygen and its radical species (Dizhbite et al., 2004; Sakagami et al., 1992). Lignin is also known as a major component in dietary fibre which can inhibit the activity of enzymes related to generation of superoxide anion radicals and obstruct the growth and viability of cancer cells (Lu et al., 1998). Therefore, due to its antioxidant activity and capacity to reduce the production of radicals and its ability to stabilize reactions induced by oxygen and its radical species, the application of lignin in cosmetic, pharmaceutical and food processing industries is promising.

Pan et al. (2006) investigated the radical scavenging activity of lignin, identifying the most important structural features of the lignin for its antiradical efficiency. This study found that the processing conditions used for the extraction of organosolv ethanol lignin influenced the structural features such as functional groups and molecular weight of the isolated lignin and consequently the antioxidant activity of lignin. In general, lignin prepared at elevated temperature, extended reaction time, increased catalyst and diluted ethanol showed higher antioxidant activity due to an increase in the number of phenolic hydroxyl groups, low molecular weight and narrow polydispersity of the lignin. The antioxidant activity and structural features of the lignin can be predicted using the regression models developed (Pan et al., 2006).

Besides, the antioxidant capacity of the lignin extracted from oil palm black liquor has been studied by Bhat et al. (2009). The antioxidant activity was characterized using 1,1-diphenyl-2-picrylhydrazyl (DPPH) as a reactive free radical method which has been widely recognized as the most reliable technique for measuring antioxidant activity (Senba et al., 1999; Dizhbite et al., 2004). The results on the percentage inhibition of DPPH radical in the isolated oil palm black liquor lignin were comparable to the earlier reports on lignin extracted from other plant sources (Vinardell et al., 2008; Ugartondo et al., 2008). Therefore, the results definitely showed that lignin obtained from oil palm waste has wide potential for use as an antioxidant compound and its use should be explored commercially (Bhat et al., 2009).

The development of oil palm EFB lignin for its application in pharmaceuticals and food industries promises an additional value to lignin. However, before oil palm EFB lignin can be developed as a nutraceutical and health supplement, the investigation of its potential in interacting with other drugs or pharmaceutical agents must be carried out to ensure product safety. This is because many dietary polyphenolic compounds undergo extensive biotransformation including oxidation, reduction, methylation, sulfation, glucuronidation and microbial degradation (Lambert and Yang, 2003; Hu et al., 2003). Therefore, oil palm EFB lignin which is composed of polyphenol compounds would have the potential to be metabolized by the same drug metabolism enzymes (DMEs) as other drugs or pharmaceutical agents.

In addition, the effect of plant extract on glutathione S-transferase (GST) activities (one of the phase II drug metabolism enzymes) was always investigated along with their antioxidant capacities, since the GST enzymes account for the

defence against oxidative stress. They detoxify endogenous harmful compounds such as the breakdown products of lipid peroxidation or DNA hydroperoxides (Hayes and Pulford, 1995; Nordberg and Arn'er, 2001). Another reason, to attract the interest on GST activity is the ability of resistant tumor cells to promote GST catalysed GSH conjugation of the pharmacologically active compounds such as antitumor drugs (Guadiano et al., 2000; van Zanden et al., 2004). In this respect, inhibitory effects of antioxidant on phase II enzymes such as GST activity are continuously investigated by researchers (Gyamfi et al., 2004).

There are two general categories of drug interaction mechanisms namely pharmacokinetics which includes absorption, distribution, metabolism and excretion of drug and pharmacodynamics which includes the combination of pharmacological effects of a drug (Ismail, 2009). Many of these interactions involved inhibition of metabolizing enzymes resulting in increased systemic exposure and subsequent adverse drug reaction. In other cases, induction of metabolizing enzymes resulted in reduced systemic exposure leading to the risk of loss of efficacy of co-administered drugs (Zhang et al., 2010). Contrary to inhibition, induction of drug metabolizing enzyme activity is a slow process because it depends on the rate of synthesis of the new enzyme and is usually noticeable after a few days or weeks (Cott, 2001). The interaction could result in food-drug interaction and may cause adverse side effects (Honig et al., 1993; Sorensen, 2002; Brandin et al., 2007).

2.4 Drug metabolizing enzymes

Drug metabolizing enzymes (DMEs) are a diverse group of proteins that are responsible for metabolizing a vast array of xenobiotic chemicals, including drugs, carcinogens, pesticides, pollutants and food toxicants, as well as endogenous

compounds, such as steroids, prostaglandins and bile acids (Coon, 2005; Brown et al., 2008; Rendic and Guengerich, 2010). Generally DMEs eliminate foreign compounds (xenobiotics) and endogenous substances by increasing solubility through the functionalization process in phase I and/or conjugation reactions in phase II.

In phase I drug metabolism, the reaction includes transformation of a parent compound to more polar metabolites by unmasking functional groups such as hydroxyl ($-OH$), amine ($-NH_2$) and sulfhydryl ($-SH$). The N- and O-dealkylation, aliphatic and aromatic hydroxylation, N- and S-oxidation and deamination are included in this reaction (Gonzalez and Tukey, 2005). In this phase, cytochrome P450 (CYP450) is the main enzyme performing mainly hydroxylation, hence acting as monooxygenases, dioxygenases and hydrolases (Gonzalez and Tukey, 2005). The addition of functional groups does little to increase the water solubility of the drug, but can dramatically alter the biological properties of the drug (Gonzalez and Tukey, 2005). The main function of phase I metabolism is to prepare the foreign compounds for phase II metabolism (Gibson and Skett 2001; Nassar, 2009).

Phase II drug metabolism reactions include conjugation reaction such as glucuronidation, sulfation, methylation, acetylation, glutathione and amino acid conjugation (Gonzalez and Tukey, 2005). Phase II metabolism enzymes are mostly transferases including UDP-glucuronosyltransferases (UGTs), sulfotransferases (SULTs), N-acetyltransferases (NATs), glutathione S-transferases (GSTs) and various methyltransferases mainly thiopurine S-methyltransferase (TPMT) and catechol O-methyl transferase (COMT) (Jancova et al., 2010).

Although the phase II reactions are so named due to their sequence of occurring following phase I modifications of a drug, a xenobiotic can undergo phase

II metabolism without prior phase I metabolism if the foreign compound has already possessed suitable functional groups and therefore can be directly metabolized through phase II enzymes before being eliminated from the body (Kaushik et al., 2006; Chen, 2012). Zidovudine, morphine and codeine are example of drugs which are metabolized primarily through UGT enzymes. The cancer chemotherapy agents such as adriamycin and thiotepa are the example of drugs which are metabolized primarily through GST enzyme (William et al., 2004; Scott and Kelly, 2003a; Scott and Kelly, 2003b; Akhdar et al., 2012).

Metabolites formed from phase II reactions have higher polarity compared to the parent drugs, thus are more readily excreted in the urine and bile. Therefore, phase II is the true ‘detoxification’ of foreign compounds to produce metabolites that are generally water-soluble and easily excreted (Lohr et al., 1998). These enzymes mostly exhibit broad substrate selectivity and eliminate many therapeutic drugs, endogenous compounds and secondary plant metabolites such as flavonoids and polyphenolic compounds (Nijveldt et al., 2001).

2.5 UDP-glucuronosyltransferase enzymes activity

The uridine 5’-diphospho-glucuronosyltransferases (UGTs) are a superfamily of protein enzymes which are responsible for metabolism of xenobiotics such as drugs, chemical carcinogens, environmental pollutants and dietary substances and endobiotics such as bilirubin, steroid hormones, thyroid hormones, bile acids and fat-soluble vitamins (Kiang et al., 2005; Jancova et al, 2010). The UGT enzymes play a major role in catalyzing a conjugation process known as glucuronidation (Jancova et al., 2010).

Figure 2.4 illustrates the conjugation reaction scheme of nucleophile substrate with uridine-5'-diphospho- α -D-glucuronic acid (UDPGA). During the glucuronidation conjugation reaction a glucose-derived moiety glucuronic acid is conjugated to a suitable functional site (hydroxyl, carboxyl, carbonyl, sulfhydryl and amine) on a substrate modulated by UGT proteins. Generally, this reaction leads to formation of the respective β -D-glucuronides with easy elimination by bile or urine (Jancova et al., 2010).

In mammalian cells, UGT superfamily can be divided into four families namely UGT1, UGT2, UGT3 and UGT8 (Mackenzie et al., 1997). However, two of the families are known to use UDPGA as sugar donors which are UGT1 (1A1, 1A3, 1A4, 1A5, 1A6, 1A7, 1A8, 1A9, 1A10) and UGT2 (2A1, 2A3, 2B4, 2B7, 2B11, 2B15, 2B2) (Court et al., 2002). However, UGT1A1, 1A3, 1A4, 1A6, 1A9, 2B7 and 2B15 appear to have the greatest importance in drug and xenobiotic metabolism (Kiang et al., 2005; Miners et al., 2010). Characterization of these isoforms based on substrate specificity is essential to understand their role in drug metabolism. In the drug metabolizing enzyme assay it is important to select suitable substrates which are specific to the enzyme for prediction of drug metabolic clearance (Miners and Birkett, 1998).

as a fungicide (Eichenbaum et al., 2009). It appears as colourless to slightly yellow crystalline solid with no odour. The *p*-NP is excreted almost exclusively as its glucuronide and sulfate conjugates (Almási et al., 2011). Because of its simple and well characterized metabolic profile, *p*-NP is widely used as a model substrate to evaluate the effect of drug therapy, disease, nutrient deficiencies and other physiologically altered conditions on conjugative drug metabolism in animal studies both *in vitro* and *in vivo* (Almási et al., 2006).

p-NP is commonly used because its colour disappearance upon glucuronidation can be followed by a colorimetric procedure (Bock et al., 1983; Embola et al., 2002). Conjugated *p*-NP is colourless and does not contribute to the colour output. Thus, the signal generated is inversely correlated with UGT activity present in the sample. This colour-changing property makes this compound useful as a marker substrate for studying UGT activity (Bock et al., 1983; Embola et al., 2002).

4-MU is a phenolic compound that is used as a drug in bile therapy. It is a crystalline solid and soluble in methanol and glacial acetic acid (Uchaipichat et al., 2004). It is used as a standard for the fluorometric determination of enzyme activity (Uchaipichat et al., 2004). Both *p*-NP and 4-MU are known as planar phenol derivatives. These compounds have been reported to be mainly conjugated by UGT1A6 isoform in mammals although the contribution ratio differed extensively among the animal species (Mackenzie et al., 1997; de Wildt et al., 1999). However, some studies had reported that *p*-NP and 4-MU were also metabolized by multiple recombinant human UGT isoforms (Tsoutsikous et al., 2004; Uchaipichat et al., 2004). Meanwhile, Yu et al. (2006) reported that recombinant rat UGT1A1,

UGT1A2, UGT1A3 and UGT1A7 isoforms showed glucuronidation activity towards 4-MU.

2.6 Glutathione S-transferase enzymes activity

Glutathione S-transferase (GST) is one of the major phase II detoxification enzymes. GST activity is present in most animal tissues. GST utilizes glutathione (GSH) to scavenge electrophilic xenobiotics as part of an organism's defence mechanism against the mutagenic, carcinogenic and toxic effects of such compounds. This is because GST enzymes account for the defence against oxidative stress and they detoxify endogenous harmful compounds such as the breakdown products of lipid peroxidation or DNA hydroperoxides (Hayes and Pulford, 1995; Nordberg and Arnér, 2001). The general mechanism for the conjugation of glutathione with xenobiotic compounds catalyzed by glutathione S-transferase enzymes is shown in Figure 2.5. Generally, GST enzymes catalyze conjugation reactions between glutathione and an electrophile compound by the formation of a thioether. This reaction generally uses 1-chloro-2,4-dinitrobenzene (CDNB) as a substrate, which can react enzymatically or non-enzymatically with the nucleophile (Jancova, 2010). Hence, the kinetics of the thioether formation can be monitored over time and the activity can be calculated (Jancova, 2010).

GST has been described by two distinct superfamilies. The first superfamily consists of soluble dimeric enzymes which are involved in biotransformation of toxic xenobiotics and endobiotics (Jancova et al, 2010). This soluble GST superfamily is subdivided into eight separate classes and designated to Alpha, Mu, Pi, Theta, Zeta, Sigma, Kappa and Omega (Jancova et al, 2010). This class is based on their gene sequence identity. These enzymes have been described mainly in cytoplasm but they